Electron orbits and stability in realizable and unrealizable wigglers of free-electron lasers

Paul Diament
Department of Electrical Engineering, Columbia University, New York, New York 10027
(Received 2 September 1980)

Magnetostatic wiggler fields $\hat{x}\cos kz + \hat{y}\sin kz$, commonly used to model the undulators of free-electron lasers, violate Maxwell's equations and are "unrealizable." Realizable wigglers that approximate the unrealizable ones near the axis have a radial variation and an axial field component, both of which affect electron motion. Exact helical equilibrium orbits are given for relativistic electrons in a combined uniform guide field and realizable wiggler, in cylindrical geometry. The parameter ka that measures the size of the helix also measures the imparted quiver motion, on which the gain of the laser depends. Hence, wigglers that impart substantial quiver motion necessarily have electrons far from the axis, for which the unrealizable wiggler model is not valid. A linearized stability analysis shows that the equilibrium helical orbits are either strongly unstable or else exhibit a secular growth, linear in time. The trajectory of an electron that starts from given position and velocity in combined guide field and wiggler is also found from the perturbation analysis, with corrections for realizability and for harmonics of practical wigglers, such as a bifilar winding. Although the helical orbits are either strongly or weakly unstable, a class of nonhelical bounded orbits is found when the secular behavior is suppressed.

I. INTRODUCTION

The pump wave of a free-electron laser[1] is often conveniently provided by a spatially periodic magnetic field, called a wiggler. Its purpose is to impart a sufficient transverse oscillatory motion to the beam electrons to interact with the radiation that is amplified. The wiggler field is commonly generated by a periodic helical winding around the drift tube, usually distinct from the coils that provide the strong axial guide field. An electron in a wiggler field is commonly thought to execute a simple helical motion with pitch corresponding to the periodicity of the imposed field.[2] The wiggler thereby acts as a pump wave for a three-wave interaction whose instability accounts for the growth of the backscattered wave and the density modulation of the relativistic electron beam. Analyses of the growth rate of this interaction have been based on perturbations of such helical electron orbits, which are equilibrium trajectories in an idealized transverse wiggler field that varies sinusoidally along the axis and has no transverse variation. What is commonly overlooked or dismissed as unimportant, however, is the fact that this idealized-wiggler field is unrealizable, because it violates Maxwell's equations. This paper addresses the question of how reliable the assumption of an unrealizable-wiggler field may be, by calculating the corrections to its electron trajectories.

Theories of the effects of wiggler fields[1-15] have been based on their description by a vector potential that is a simple periodic function of axial distance alone. This leads to a very simple magnetic field and to the consequence that the transverse canonical momenta are constants of the motion in the absence of a uniform guide field. The resultant electron trajectories conforming to these constants are simple helices and integration along such orbits can serve to deduce growth rates of the free-electron laser instability, among other quantities of interest.

The fallacy in such analyses is that the wiggler fields or potentials that have been used fail to satisfy all the requirements of Maxwell's equations. Although the wiggler field is solenoidal, it is not irrotational and can hence not be generated by any windings, in the absence of a nonphysical configuration of currents that would fill the entire space in which the wiggler field is to be set up. Such wiggler fields are hence unrealizable.

Realizable versions of the wiggler field have transverse as well as axial dependence and also an axial field component. Consequently, the transverse momentum is not a constant of the motion even without a guide field and the electron orbits are distorted from their idealized spiral. The stability and growth rates of the system are affected.

As corrections to the motion in an unrealizable-wiggler field are sought, it is also appropriate to investigate the further perturbations that arise in practical, rather than idealized, versions of wigglers. They may be generated by a winding such as a bifilar helix[16] around the drift tube, rather than the ideal sinusoidal surface current. Such windings generate harmonics of the fundamental periodic field and these further distort the motion of the electrons.

The justification for the widespread use of the unrealizable wiggler, besides its simplicity, is that it is an approximation to the correct field pattern near the axis of the system. There is

hence a need to determine how far from the axis an electron may get before the approximation becomes unacceptable.

In this paper, both the ideal and practical versions of realizable-wiggler fields are considered, in their full cylindrical geometry. The realizable wiggler is treated as the simple unrealizable one, augmented by a correction field that may be considered a small perturbation of the improper system. The unrealizable wiggler's axial field gradient cannot be neglected in applying perturbation theory to obtain the corrected orbits. A uniform axial guide field is included in the calculations, which are analytic throughout and fully relativistic.

The limitations of the calculations presented herein are that they apply to single-particle motion in infinitely long wigglers and that, except for the exact helical orbits, they are based on linearized equations of motion. What emerges, however, are corrections to the improper equilibrium orbit in the unrealizable-wiggler field, the stability of that equilibrium, and the transient motion from any given initial position and velocity of the electron.

In brief, the results will demonstrate that, firstly, the unrealizable-wiggler approximation is unacceptable whenever the wiggler does impart a significant transverse oscillation to the electron, as it is designed to do, because it then also causes it to travel significantly far from the axis. Secondly, the unrealizable-wiggler equilibria are shown to be at least weakly unstable, within the linearized regime. It is also shown that helical equilibria can exist, but with a radius and initial conditions different from those obtained for the unrealizable wiggler. There is also a class of nonhelical trajectories whose motion is bounded. The results shed light on observations of beam spreading and can help in designing useful wiggler configurations. Since collective behavior in a beam, including growth rates of the wave interactions, are obtainable by suitable integration along particle trajectories, the corrections to the unrealizable-wiggler electron orbits can serve to advance the theory of operation of free-electron lasers.

II. WIGGLER FIELDS

A. Unrealizable wiggler

The prototype of the wiggler field is a unit vector that varies periodically in direction along the z axis, with period $2\pi/k$:

$$\hat{w}(kz) = \hat{x}\cos kz + \hat{y}\sin kz\,. \tag{1}$$

As one progresses along the z axis, this vector is observed to rotate uniformly about the axis; it is circularly polarized. The function $\hat{w}(\theta)$ satisfies the differential equation

$$\frac{d\hat{w}(\theta)}{d\theta} = \hat{z}\times\hat{w}(\theta)\,, \tag{2}$$

which implies precession. In cylindrical coordinates, the wiggler field is

$$\hat{w}(kz) = \hat{r}\cos(kz-\phi) + \hat{\phi}\sin(kz-\phi)\,. \tag{3}$$

The wiggler magnetic field is proportional to $\hat{w}(kz)$ and when a uniform axial guide field is superimposed, the combination is expressed by

$$(e/m)\vec{B}(z) = \omega_0\hat{w}(kz) + \omega_c\hat{z}\,. \tag{4}$$

The magnetic field lines are helical. The cyclotron frequency, in the laboratory frame, of the uniform axial field is ω_c and the corresponding frequency for the amplitude of the sinusoidal transverse field is ω_0; m and $-e$ are the rest mass and charge of an electron.

This wiggler magnetic field is derived from the vector potential

$$(e/m)\vec{A}(z) = -(\omega_0/k)\hat{w}(kz)\,, \tag{5}$$

exclusive of the axial guide field; i.e., the wiggler's vector potential is of the same form as the wiggler itself.

It is clear, however, that this magnetic field is unrealizable by any set of coils or windings outside of the space in which the field is to be generated. Since $\vec{B}$ is the curl of a vector potential of the same form, its own curl is also of that form and cannot vanish. The wiggler magnetic field can hence exist only in the presence of a volume distribution of current of density $\vec{J}$ given by

$$(\mu_0 e/m)\vec{J}(z) = \vec{\nabla}\times(e/m)\vec{B} = -\omega_0 k\hat{w}(kz) \tag{6}$$

throughout the space occupied by the wiggler field. No such current distribution is present, of course, within the drift tube where the wiggler field is desired. Nor does the wiggler field become more realistic in the presence of a beam of electrons, not only because the flow implied by $\vec{J}$ includes no axial flow but also because the current is opposite in direction to that of a distribution of electrons gyrating in the wiggler field, in accordance with Lenz' law. Thus, no distribution of electrons, with or without accompanying ions, can make this wiggler field self-consistent. The wiggler is truly unrealizable.

Why, then, is this field used so commonly in analyses of free-electron lasers? Besides the simplicity of the periodic, circularly polarized wiggler field and the fact that the field is just proportional to its potential, the property of dependence on only the axial coordinate z implies that the transverse components of the canonical

momentum are constants of the motion. Combining this with the constancy of the particle energy fully determines the particle orbits in a simple way and greatly facilitates the further analysis of beams, collective effects, and wave interactions. The justification for considering the unrealizable-wiggler field, despite the violation of Maxwell's equations, is that it does exist on the axis of an appropriate helically wound solenoid and is an approximately correct description of its field close to the axis. How far from the axis one may get before the approximation breaks down is an important question to be resolved.

B. Realizable wiggler

A wiggler magnetic field configuration that can be realized within a region by appropriate surface currents surrounding the region must be both solenoidal and irrotational. The field may be derived from a potential that satisfies Laplace's equation within the region. The potential field may be either a vector potential,

$$\vec{B}=\vec{\nabla}\times\vec{A}\,,\quad \nabla^2\vec{A}=0\,, \tag{7}$$

or a scalar potential (except at the source winding itself),

$$(e/m)\vec{B}=\vec{\nabla}\psi\,,\quad \nabla^2\psi=0\,. \tag{8}$$

If the region is cylindrical and the axial variation is to be sinusoidal, then the radial variation is that of a modified Bessel function. The field that reduces to the unrealizable wiggler when evaluated exactly on the axis of the cylindrical space is derived from

$$\psi(r,\phi,z)=2(\omega_0/k)I_1(kr)\cos(\phi-kz)+\omega_c z \tag{9}$$

or, if the vector potential is preferred, from $(e/m)\vec{A}=\hat{z}\times\vec{\nabla}M$ with

$$M(r,\phi,z)=2(\omega_0/k^2)I_1(kr)\sin(\phi-kz)+\omega_c r^2/4\,. \tag{10}$$

These represent a single cylindrical harmonic, in the sourceless region up to the radius $r=b$ where the source winding or surface current is located.

The realizable-wiggler vector potential is given by

$$(e/m)A_r=-(\omega_0/k)[2I_1(kr)/kr]\cos(\phi-kz)\,, \tag{11}$$

$$(e/m)A_\phi=(\omega_0/k)[2I_1'(kr)]\sin(\phi-kz)+\omega_c r/2\,, \tag{12}$$

and its magnetic field is

$$(e/m)B_r=\omega_0 2I_1'(kr)\cos(\phi-kz)\,, \tag{13}$$

$$(e/m)B_\phi=-\omega_0 2[I_1(kr)/kr]\sin(\phi-kz)\,, \tag{14}$$

$$(e/m)B_z=\omega_0 2I_1(kr)\sin(\phi-kz)+\omega_c\,. \tag{15}$$

Since $I_1(x)\to x/2$ as $x\to 0$, the realizable-wiggler field does approach the unrealizable one as $r\to 0$. Near the axis, the lowest-order correction terms to the unrealizable field vary quadratically with radius for the transverse components and linearly for the axial one. Up to cubic terms,

$$(e/m)\vec{B}_\perp-\omega_0\hat{w}(kz)=(\omega_0/8)k^2r^2[\hat{r}3\cos(\phi-kz)-\hat{\phi}\sin(\hat{\phi}-kz)]\,, \tag{16}$$

$$(e/m)\vec{B}_\parallel-\omega_c\hat{z}=\omega_0\hat{z}(kr+k^3r^3/8)\sin(\phi-kz)\,. \tag{17}$$

The full corrections to $\omega_0\hat{w}(kz)+\omega_c\hat{z}$ are

$$\Delta(e/m)B_r=\omega_0[I_0(kr)-1+I_2(kr)]\cos(\phi-kz)\,, \tag{18}$$

$$\Delta(e/m)B_\phi=-\omega_0[I_0(kr)-1-I_2(kr)]\sin(\phi-kz)\,, \tag{19}$$

$$\Delta(e/m)B_z=\omega_0 2I_1(kr)\sin(\phi-kz)\,. \tag{20}$$

Consequently, ω_0 should be more precisely defined as the laboratory-frame cyclotron frequency corresponding to the purely sinusoidal transverse field amplitude as measured on the axis; the field strength is a function of radius

$$[(e/m)B_\perp]_{\rm rms}=\omega_0[I_0^2(kr)+I_2^2(kr)]^{1/2}\,, \tag{21}$$

so that measurements of transverse-wiggler-field strength made off-axis should be corrected accordingly to arrive at ω_0.

C. Practical wigglers

Wiggler magnetic fields are commonly generated by periodic helical windings at radius b outside the drift tube. The ideal wiggler source current is free of harmonics and constitutes a sinusoidal surface current sheet at the surface $r=b$. Since the radial component of magnetic field must be continuous across this surface, the scalar potential outside the winding is

$$\psi(r,\phi,z)=2(\omega_0/k)[I_1'(kb)/K_1'(kb)]K_1(kr)\cos(\phi-kz)\,, \tag{22}$$

for $r>b$, instead of Eq. (9) for $r<b$. The fields outside are as in Eqs. (13)–(15), but with $I_1(kr)$ replaced by

$$[I_1'(kb)/K_1'(kb)]K_1(kr)$$

and without ω_c. The source current density is given by the discontinuity in tangential field

$$\mu_0(e/m)\vec{K}(\phi,z)=\hat{r}\times[(e/m)\vec{B}_{\rm out}-(e/m)\vec{B}_{\rm in}]=\hat{\phi}\omega_c+(\hat{\phi}+\hat{z}/kb)(\omega_0/\xi_1)\sin(\phi-kz)\,, \tag{23}$$

where

$$\xi_1=[-kbK_1'(kb)]/2=[kbK_0(kb)+K_1(kb)]/2\,. \tag{24}$$

Besides the simple solenoid that generates the guide field ω_c, this surface current involves a

helical sinusoidal flow, periodic with pitch $2\pi/k$, directed at angle $\tan^{-1}(kb)$ to the axis.

The sinusoidal surface current sheet is, of course, an idealization. In practice, a periodic winding carrying concentrated currents approximates the current sheet, in the sense that the fundamental component of the Fourier series that represents the periodic current distribution can correspond to the ideal current sheet. An example is the conventional bifilar winding,[15] which is a double helical winding with equal and opposite currents I_B in wires spaced a half-period apart, with pitch $2\pi/k$. Assuming the uniform static magnetic field is generated by a tightly wound solenoid separate from the wiggler winding, the combined source current can be expressed as

$$\vec{K}(\phi,z)=K_c\hat{\phi}+\left(\hat{\phi}+\frac{\hat{z}}{kb}\right)I_B k\sum_l K_B(\phi-kz-l2\pi)\,, \quad (25)$$

where $\mu_0(e/m)K_c=\omega_c$ gives the uniform field, the summation over all integers makes the source periodic, and the surface current for a single period of the bifilar helix is

$$K_B(\phi-kz)=\delta(\phi-kz-\pi/2)-\delta(\phi-kz+\pi/2)\,, \quad (26)$$

if the concentrated currents in the wires are represented by delta-function surface distributions.

To obtain the magnetic field generated by any such winding, it is convenient to express the periodic surface current as a Fourier series in the helical coordinate ϕ-kz, because each Fourier component of the source current generates a field given by the corresponding cylindrical harmonic. For the bifilar helix, the Fourier series is

$$\sum_l K_B(\phi-kz-l2\pi)=\frac{2}{\pi}\sum_{n>0}\sin(n\pi/2)\sin n(\phi-kz)\,, \quad (27)$$

where the origin has been located midway between neighboring wires; only odd harmonics are present. The field generated by any surface current with a Fourier series given by arbitrary coefficients Q_n as in

$$\mu_0\left(\frac{e}{m}\right)\vec{K}=\omega_c\hat{\phi}+\omega_0\left(\hat{\phi}+\frac{\hat{z}}{kb}\right)\sum_{n>0}Q_n\sin n(\phi-kz)\,, \quad (28)$$

is derivable as in Eq. (8) from a scalar potential with corresponding series

$$\psi(r,\phi,z)=\omega_c z+\frac{2\omega_0}{k}\sum_{n>0}\frac{\xi_n}{n}Q_n I_n(nkr)\cos n(\phi-kz)\,, \quad (29)$$

where

$$\xi_n=[-nkbK_n'(nkb)]/2=[nkbK_{n-1}(nkb)+nK_n(nkb)]/2\,. \quad (30)$$

The fundamental component, $n=1$, reduces to the unrealizable-wiggler potential near the axis, provided that $Q_1=1/\xi_1$. For the case of the bifilar helix, this requires a current

$$I_B=(\omega_0/kc)I_{17}/8\xi_1\,, \quad (31)$$

in each helix, where

$$I_{17}=4\pi\epsilon_0 mc^3/e=17.0\text{ kA}.$$

As an example, for a wiggler of 8-cm period and 2-cm radius to provide a transverse magnetic field of 500 G on axis (i.e., to achieve $\omega_0=1.4$ GHz with $kc=3.75$ GHz and $kb=1.57$) would require $I_B=2.85$ kA in the bifilar winding. It is important to note that the required current increases roughly exponentially as the radius of the winding increases; it can easily get prohibitively large if kb is not kept of order unity.[16]

For a general winding of radius b and period $2\pi/k$, with Fourier spectrum Q_n as in Eq. (28), the magnetic field generated within the enclosed space will be that of an unrealizable wiggler, plus two corrections. One correction is to the fundamental Fourier component, as required to satisfy Maxwell's equations and already presented above in Eqs. (18)–(20). The other correction field is comprised of the inevitable harmonics for any practical coil configuration. The field is

$$(e/m)\vec{B}=[\omega_0\hat{w}(kz)+\omega_c\hat{z}]+\omega_0\vec{\Omega}(kr,\phi-kz)\,, \quad (32)$$

with correction fields

$$\vec{\Omega}(\eta,\theta)=\vec{\Omega}^1(\eta,\theta)+\sum_{n>1}\vec{\Omega}^n(\eta,\theta)\,, \quad (33)$$

given by the fundamental

$$\Omega_r^1(\eta,\theta)=[I_0(\eta)-1+I_2(\eta)]\cos\theta\,, \quad (34)$$

$$\Omega_\phi^1(\eta,\theta)=-[I_0(\eta)-1-I_2(\eta)]\sin\theta\,, \quad (35)$$

$$\Omega_z^1(\eta,\theta)=2I_1(\eta)\sin\theta\,, \quad (36)$$

and the harmonics

$$\Omega_r^n(\eta,\theta)=\xi_n Q_n[I_{n-1}(n\eta)+I_{n+1}(n\eta)]\cos n\theta\,, \quad (37)$$

$$\Omega_\phi^n(\eta,\theta)=-\xi_n Q_n[I_{n-1}(n\eta)-I_{n+1}(n\eta)]\sin n\theta\,, \quad (38)$$

$$\Omega_z^n(\eta,\theta)=\xi_n Q_n 2I_n(n\eta)\sin n\theta\,. \quad (39)$$

Both the radial dependence of the correction field and the oscillatory axial field component will be seen to affect the electron dynamics significantly.

In the preceding formulas, the wiggler winding has been assumed to have zero average current, so that its Fourier series has no dc term. If a winding is not balanced to zero net current per period, the resulting uniform field simply affects the value of ω_c. Also, the origin of the helical coordinate ϕ-kz has been chosen to give the wind-

ing odd symmetry, making the cosine Fourier components superfluous.

III. ELECTRON MOTION IN WIGGLERS

A. Unrealizable wiggler

Consider a single electron moving in a combined wiggler and uniform guide field. In a magnetostatic field, the total energy remains constant at its initial value but there is some division of the available energy between axial and transverse motions. In the uniform field, the axial drift and transverse gyration combine into a helical orbit about some rectilinear guiding center. With the addition of the wiggler field, a helical orbit is still allowable, as will be seen, but with its pitch determined by the period of the wiggler and the gyration radius affected by both the wiggler and guide field strengths. For the case of the unrealizable wiggler, which is independent of the transverse coordinates, the location of the guiding center is arbitrary.

To account fully for relativistic effects, it is simplest to use the proper time τ in the equation of motion that governs the orbit $\vec{r}(\tau)$

$$\frac{d^2\vec{r}}{d\tau^2}=\frac{e}{m}\vec{B}(\vec{r})\times\frac{d\vec{r}}{d\tau}. \tag{40}$$

The observed time coordinate is just proportional to the proper time,

$$t=\gamma\tau, \tag{41}$$

since the total energy γmc^2 remains constant. The constant magnitude of the velocity is given by

$$\left(\frac{d\vec{r}}{d\tau}\right)^2=\gamma^2\beta^2c^2, \tag{42}$$

where βc is the observed speed and, as usual,

$$\gamma^2\beta^2=\gamma^2-1 \tag{43}$$

to satisfy the principle of relativity.

We develop the theory[11,14,15] of helical motion in combined wiggler and guide fields, in terms of orbital position rather than velocity alone. In Eq. (40), the magnetic field is $\vec{B}(\vec{r}(\tau))$, evaluated at the location of the electron. For the unrealizable wiggler

$$(e/m)\vec{B}^0=\omega_c\hat{z}+\omega_0\hat{w}(kz), \tag{44}$$

this depends only on z. We assume uniform axial motion $z=u\tau$, which means an observed axial velocity u/γ, and we seek spiral motion of some radius a about a guiding center line through $\vec{r}_0$, with the period of the wiggler.

$$\vec{r}(\tau)=\vec{r}_0+u\tau\hat{z}+a\hat{z}\times\hat{w}(ku\tau). \tag{45}$$

This way of expressing the orbit gives the velocity a form similar to that of the magnetic field, because of Eq. (2) and $\hat{z}\times(\hat{z}\times\hat{w})=-\hat{w}$

$$\frac{d\vec{r}}{d\tau}=u\hat{z}-kau\hat{w}(ku\tau). \tag{46}$$

The acceleration

$$\frac{d^2\vec{r}}{d\tau^2}=-ka\,ku^2\hat{z}\times\hat{w}(ku\tau), \tag{47}$$

is to be equated to that imposed by the magnetic field at $z(\tau)=u\tau$:

$$\frac{e}{m}\vec{B}^0\times\frac{d\vec{r}}{d\tau}=[\omega_c\hat{z}+\omega_0\hat{w}(ku\tau)]\times[u\hat{z}-kau\hat{w}(ku\tau)]$$

$$=-u(\omega_0+\omega_c ka)\hat{z}\times\hat{w}(ku\tau). \tag{48}$$

The assumed helical orbit is seen to be consistent with the equation of motion, provided the axial speed and the gyration radius are related by

$$ku=\omega_c+\omega_0/ka. \tag{49}$$

However, these same two parameters are already constrained by Eq. (42) to satisfy

$$\left(\frac{d\vec{r}}{d\tau}\right)^2=u^2(1+k^2a^2)=\gamma^2\beta^2c^2, \tag{50}$$

so that

$$ku=\gamma\beta kc/(1+k^2a^2)^{1/2} \tag{51}$$

relates the drift and gyration to the electron energy. Combining Eq. (49) and Eq. (51) shows that the axial speed and gyration radius are determined by two adjustable parameters, the pump strength

$$p=\omega_0/\omega_c, \tag{52}$$

or ratio of transverse to axial field amplitudes, and the energy parameter

$$g=\gamma\beta kc/\omega_c, \tag{53}$$

which compares the relativistically Doppler-shifted spatial frequency of the wiggler to the cyclotron frequency of the guide field. The gyration radius is given by a quartic equation for ka, obtained by eliminating ku,

$$k^4a^4+2pk^3a^3+(1+p^2-g^2)k^2a^2+2pka+p^2=0, \tag{54}$$

and the axial motion is then determined by

$$ku/\omega_c=1+p/ka. \tag{55}$$

In case the guide field is absent ($\omega_c=0$), the normalization to the cyclotron frequency is inappropriate and the two relations are replaced by

$$(ku/\omega_0)^2=(\gamma\beta kc/\omega_0)^2-1=1/k^2a^2. \tag{56}$$

Before exploring the quartic Eq. (54) that gives the basic characteristic of the wiggler/guide system, the interpretation of the parameters must be

clearly delineated. Because the unit vectors $\hat{w}(ku\tau)$ and $\hat{z}\times\hat{w}(ku\tau)$ rotate uniformly, the orbit in Eq. (45) involves uniform axial drift and uniform rotation about a rectilinear guiding center. These combine into a helical orbit, of pitch $2\pi/k$ and gyration radius a. The magnetic field lines are also helical, but the two helices do not correspond. At axial distance z, the field line of the unrealizable wiggler points along $\hat{z}+p\hat{w}(kz)$ while the electron orbit is directed along $\hat{z}-ka\hat{w}(kz)$; by Eq. (55), these directions must differ. The electron does not follow a field line; if it did, it would be unaccelerated and yet its trajectory would not be rectilinear.

It is vital to realize that the parameter ka has a dual physical significance. On the one hand, it gives the size of the circle of gyration, as projected onto a transverse plane, in relation to the period of the wiggler or pitch of the helix: It is the ratio of the circumference of this circle to the wiggler period. On the other hand, the axial velocity of the electron is $dz/dt=u/\gamma$ while the transverse velocity is, from Eq. (46) and Eq. (41), kau/γ, so that ka is also the ratio of transverse to axial velocity; $(ka)^2$ gives the division of the available energy between transverse and axial motion.

In its latter interpretation, the wiggler has performed its function of imparting a transverse quiver velocity to the electron when the velocity ratio $ka=\beta_\perp/\beta_z$ is not too small. On the basis of the former interpretation, however, ka measures the transverse displacement of the electron from its guiding center, normalized to the wiggler period. When the guiding center lies on the wiggler axis, the argument kr of the Bessel functions that give the magnetic field's radial variation as in Eqs. (13)–(15) is exactly ka; when the guiding center is off-axis, the apogee of the electron orbit is at a value of kr that exceeds ka. But kr, and hence ka, is required to remain small for the electron to sense a field that approximates the unrealizable wiggler. The contradiction in the requirements on the size of the quiver parameter ka is what renders any analysis based entirely on an unrealizable wiggler at least potentially suspect and makes it important to determine at what values of ka such analyses begin to break down.

The generality of the characteristic equation (54) is enhanced when it is realized that ka is an algebraic quantity; negative values of ka are as significant as positive ones. The radius of gyration in Eq. (45) should be understood to be $|a|$; a negative value of a merely shifts the phase along the helical orbit by a half-period, since $\hat{w}(ka+\pi)=-\hat{w}(kz)$. Even the wiggler wave number k can be assigned an algebraic sign. The vectors $\hat{w}(-kz)$ and $\hat{w}(kz)$ rotate in opposite directions. The helical coordinate ϕ-kz has right-handed helicity for positive k, while negative values of k represent a left-handed helix. Similarly, both ω_c and ω_0 can have a physically significant sign, specifying the direction of the guide field along the axis and the sense of the wiggler winding. Thus, both p and g, as well as ka, are signed quantities; however, γ and β must be considered essentially positive quantities.

Considering the quartic Eq. (54) to give ka as a function of pump strength $p=\omega_0/\omega_c$, with electron energy $g=\gamma\beta kc/\omega_c$ as a fixed parameter, the characteristic curves pass through the origin with slopes $d(ka)/dp=1/(-1\pm g)$ and are asymptotic to $ka=-p\pm g$. There are two branches, corresponding to the two signs of the square root in Eq. (51), implying two signs for u, or axial motion either forward or backward along the axis. For $g<1$, ka and p have opposite signs and there are just two values of ka for each pump strength, one for each direction of axial drift. For $g>1$, one branch has a positive slope near the origin and there can be as many as four allowable values of ka, for sufficiently small pump strengths. From the inversion of Eq. (54) to give p as $p(ka,g)$ in the form

$$p=-ka[1\pm g/(1+k^2a^2)^{1/2}], \tag{57}$$

it is readily found that the pump peaks as a function of ka for

$$(ka)_*=(g^{2/3}-1)^{1/2} \tag{58}$$

at

$$p_*=(g^{2/3}-1)^{3/2}=(ka)_*^3, \tag{59}$$

beyond which there are only two solutions, rather than four. The transition point $g=1$, at which the Doppler-shifted spatial frequency equals the cyclotron frequency of the guide field, is termed magnetoresonance. Since the total energy is a fixed quantity, nothing spectacular happens to the electron at this point. However, the resonant branch of the characteristic curve begins with infinite slope when $g=1$. This gives rather large values of ka for even small pump strengths; near zero, $ka\simeq-(2p)^{1/3}$.

Figure 1 shows plots of the characteristic equation for an unrealizable wiggler, both below and above magnetoresonance. The quiver parameter ka is plotted against pump strength $p=\omega_0/\omega_c=B_\perp/B_z$, for two fixed values of magnetization $g=\gamma\beta kc/\omega_c$. The solid curves are for $g=2.0$ and the dashed ones for $g=0.8$. The steeper branches are for $ku>0$, i.e., right-handed helical motion. Typical parameters of a wiggler system might involve a wiggler of 2 cm period and peak $B_\perp$ on axis of 500 G, with a 10-kG guide field and elec-

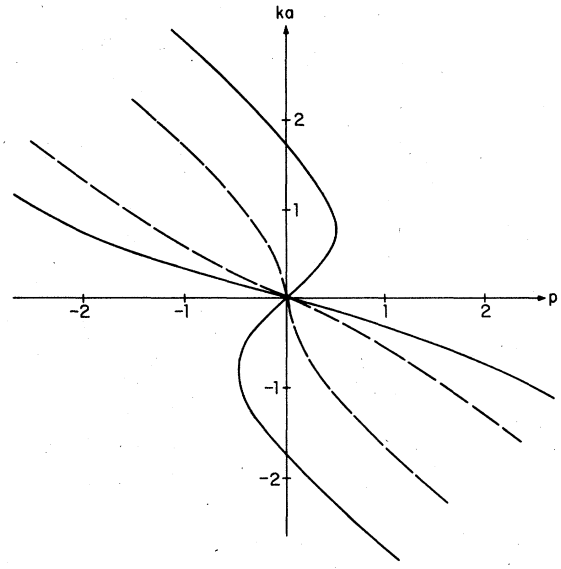

FIG. 1. Quiver parameter ka vs pump strength $p = \omega_0/\omega_c$ for an unrealizable wiggler with guide field, for $g = \gamma\beta kc/\omega_c = 2.0$ (solid) and 0.8 (dashed).

trons accelerated by 511 kV. These correspond to $kc = 15$ GHz, $\omega_0 = 1.4$ GHz, $\omega_c = 28$ GHz, and $\gamma = 2$. Hence, $g = 0.928$ and $p = 0.05$, for which the characteristic equation yields $ka = -0.379$ for forward drift and $ka = -0.0259$ for backward motion. For the former, $\beta_z = 0.810$ and $\beta_\perp = 0.307$, while for the latter, the motion is almost entirely axial, with $\beta_\perp = 0.0225$, $\beta_z = 0.866 \cong \beta$.

Since the unrealizable wiggler is a justifiable construct only at radii such that kr is small, the characteristic equation and the curves shown can be considered reliable only in the region of small values of ka. The nature of the deviations from these results when ka gets large will now be explored.

B. Realizable wiggler

In a realizable wiggler, electron motion differs from the above results because of both the radial gradient and the axial field component. Yet, a helical orbit with its guiding center along the wiggler axis can still be an exact equilibrium orbit. The electron's location at proper time τ is now expressed in terms of a rotating unit vector with arbitrary initial azimuth θ:

$$\vec{r} = u\tau\hat{z} + a\hat{w}(ku\tau + \theta) . \tag{60}$$

This implies cylindrical coordinates $r = a$, $\phi = ku\tau + \theta$, $z = u\tau$, and a helical coordinate $\phi - kz$ fixed at θ along the orbit. For the unrealizable case, θ was set at $\pi/2$ to conform to the magnetic field. The velocity along the trajectory is now

$$\frac{d\vec{r}}{d\tau} = u\hat{z} + ka u\hat{z} \times \hat{w}(ku\tau + \theta) , \tag{61}$$

and the acceleration is

$$\frac{d^2\vec{r}}{d\tau^2} = -k^2u^2a\hat{w}(ku\tau + \theta) , \tag{62}$$

which is directed radially inward.

The general combination of a uniform guide field and a wiggler derived from a helically symmetric potential $\psi(r, \phi - kz)$ has the form

$$(e/m)\vec{B} = \omega_r\hat{r} + \omega_\phi\hat{\phi} + (\omega_c - kr\omega_\phi)\hat{z} , \tag{63}$$

where

$$\omega_r = \partial\psi/\partial r, \quad \omega_\phi = \partial\psi/r\partial\phi .$$

Along the electron trajectory, this becomes

$$(e/m)\vec{B} = \omega_r(a, \theta)\hat{w} + \omega_\phi(a, \theta)\hat{z} \times \hat{w} + [\omega_c - ka\omega_\phi(a, \theta)]\hat{z} , \tag{64}$$

where $\hat{w} = \hat{w}(ku\tau + \theta)$ again. The cross product of Eq. (64) and Eq. (61) shows that the acceleration imparted to the electron is equal to that in Eq. (62) provided the following two conditions are satisfied:

$$\omega_r(a, \theta) = 0 , \tag{65}$$

$$ku = \omega_c - (ka + 1/ka)\omega_\phi(a, \theta) . \tag{66}$$

The first condition states that the radial component of the magnetic field must vanish along the helical orbit. In the second condition, ω_ϕ/ka is the transverse field contribution and $ka\omega_\phi$ is that of the axial component, which was neglected in the case of the unrealizable wiggler. In fact, the two conditions in Eqs. (65)–(66) were satisfied in Eq. (49) for the unrealizable wiggler, which is based on

$$\omega_r = \omega_0\cos\theta , \quad \omega_\phi = -\omega_0\sin\theta , \quad \omega_z = \omega_c , \tag{67}$$

by neglecting the axial component $ka\omega_\phi$ and fixing θ at $\pi/2$ to annihilate the radial component along the helix.

For the ideal realizable wiggler without harmonics, the field components along the helix are

$$\omega_r = \omega_0 2I_1'(ka)\cos\theta , \tag{68}$$

$$\omega_\phi = -\omega_0[2I_1(ka)/ka]\sin\theta , \tag{69}$$

$$\omega_z = \omega_c + \omega_0 2I_1(ka)\sin\theta , \tag{70}$$

so that $\theta = \phi - kz$ must again be fixed at $\pi/2$ to satisfy Eq. (65), or else at $-\pi/2$, which is equivalent to allowing for negative values of ka. The axial motion is then given by

$$ku = \omega_c + (ka + 1/ka)[2I_1(ka)/ka]\omega_0 , \tag{71}$$

which should be compared to Eq. (49) for the un-

realizable wiggler. Since the energy condition still dictates Eq. (51), the exact characteristic equation for an ideal realizable wiggler becomes

$$p = -kaF(ka)[1 \pm g/(1+k^2a^2)^{1/2}], \tag{72}$$

instead of Eq. (57), with the correction factor

$$F(ka) = ka/[2I_1(ka)(1+k^2a^2)]. \tag{73}$$

This factor approaches unity as $ka \to 0$, reverting to the case of the unrealizable wiggler, but it is a roughly exponentially decaying factor when ka gets large. Note that the correction to Eq. (57) involves more than merely increasing the effective value of ω_0 from its magnitude on axis to that corresponding to the transverse field at radius a. That approach would still ignore the effects of the axial field component.

Figure 2 presents plots of the exact characteristic equation for the ideal realizable wiggler, giving the quiver parameter as a function of pump strength measured on axis, for the same magnetization parameters used in Fig. 1, $g = 2.0$ (solid) and $g = 0.8$ (dashed). Comparing the realizable and unrealizable cases, it is evident that the curves differ markedly as soon as the quiver parameter attains even modest values, of the order of 0.25. The asymptotes are completely different, as large quiver parameters $ka = \beta_\perp/\beta_z$ are allowable at fixed total energy only for slow axial drift, which demands only a weak wiggler. Consequently, exactly helical orbits can be sustained in a wiggler/guide field combination only for sufficiently weak pump strengths, contrary to the unrealizable-wiggler result. For large ratios of wiggler to guide field strengths, the available energy is insufficient to allow both the axial and transverse motions that would be consistent with the combined magnetic field. A further consequence of this is that the number of allowable values of the quiver parameter can be six or none, in addition to the two or four permitted by the unrealizable field.

In case the guide field is absent, $\omega_c = 0$ and the appropriate normalization of wiggler strength is the parameter $\omega_0/\gamma\beta kc$. The exact characteristic equation for the ideal realizable wiggler is then

$$\omega_0/\gamma\beta kc = k^2a^2/[(1+k^2a^2)^{3/2}2I_1(ka)], \tag{74}$$

which may be compared with Eq. (56) for the unrealizable wiggler. Figure 3 shows ka plotted against $\omega_0/\gamma\beta kc$ for the exact case (solid lines) and the unrealizable one (dashed line). The curves are similar to those in Fig. 2, for which there is a uniform guide field, but exhibit the symmetry that is lacking when $\omega_c \neq 0$. There is a peak value of wiggler strength at a finite ka, unlike the case of the unrealizable wiggler. Beyond $\omega_0/\gamma\beta kc = 0.369$ at $ka = 0.652$, there is insufficient energy to permit any helical orbit of the required periodicity. For weaker wigglers, the allowed helix may have either a small or a large radius, instead of a unique one, for either direction along the axis.

It is clear that calculations of the performance

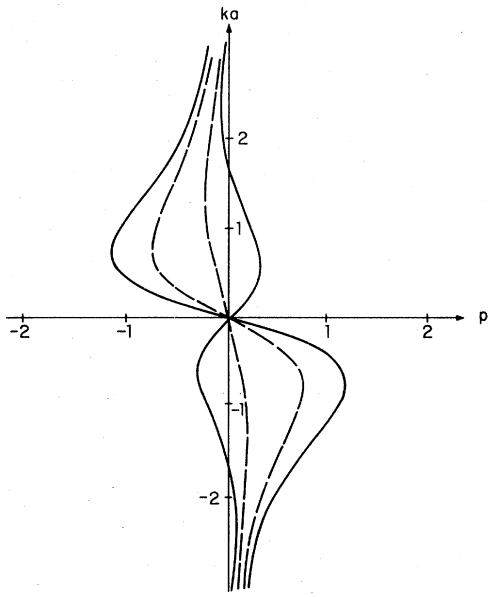

FIG. 2. Quiver parameter ka vs pump strength $p = \omega_0/\omega_c$ for an ideal realizable wiggler with guide field, for $g = \gamma\beta kc/\omega_c = 2.0$ (solid) and 0.8 (dashed).

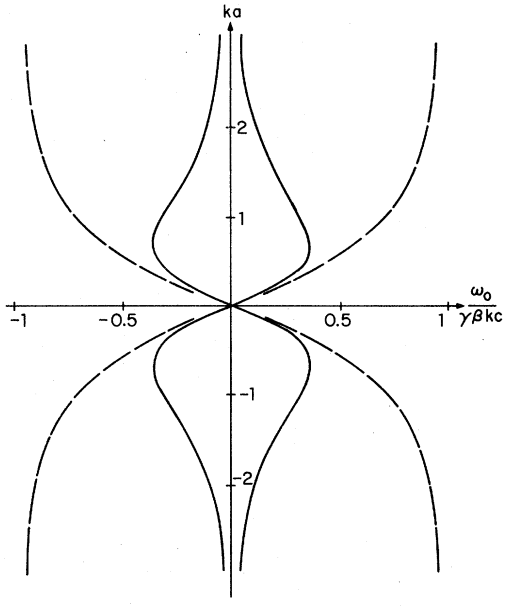

FIG. 3. Quiver parameter ka vs pump strength $\omega_0/\gamma\beta kc$ for the realizable wiggler (solid) and the unrealizable wiggler (dashed), in the absence of a uniform magnetic guide field.

of a wiggler system based only on unrealizable fields can be relied upon only if conditions are such that the quiver parameter ka is kept quite small. In the literature on this subject, the transverse motion imparted by the wiggler is often cited but is has not been recognized that the quiver parameter also measures the size of the helical orbit. Imparting substantial transverse velocities implies electron excursions far from the axis; as is usually conceded, the wiggler model used is valid only near the axis. Friedland and Hirshfield[11] illustrate their work on the effect of the uniform field on free-electron laser gain with a case of $(\gamma\beta kc/\omega_0)^2 = 99$ at which the critical magnetization implies that a quiver parameter $(ka)_* = 0.525$ is contemplated. This is now seen to be beyond the limits of applicability of the unrealizable-wiggler theory. Davidson *et al.*[12] consider a wiggler without the guide field, at $(\gamma\beta kc/\omega_0)^2 = 3$, for which $ka = 0.707$ for an unrealizable wiggler, and also at $(\gamma\beta kc/\omega_0)^2 = 75$, for which $ka = 0.116$. The latter seems small enough for the assumption of the unrealizable-wiggler field to be harmless but the former is clearly not acceptable; the realizable wiggler has no helical equilibrium for $(\gamma\beta kc/\omega_0)^2$ less than 7.34. Bernstein and Friedland[15] discuss illustrative cases with $(\gamma\beta kc/\omega_0)^2 = 32$. Without the guide field, this implies a quiver parameter $ka = 0.18$, which is tolerable. The corresponding critical guide field mentioned, however, is such that $p_* = 0.312$ and $(ka)_* = 0.678$, which invalidates the unrealizable wiggler. The rest of their illustrations deliberately maintain $ka = 0.18$, however.

Another way to illustrate the limited range of applicability of the expressions for the unrealizable wiggler is to replot its characteristic equation as a relation between axial velocity β_z and magnetization ω_c/kc, for given energy γ and pump strength ω_0/kc. This is the form presented by Friedland,[11,13-15] based on the unrealizable wiggler. Figure 4 gives this form of the characteristic curve for the realizable (solid curve) and unrealizable (dashed curve) wigglers for $\omega_0/kc = 0.5$ and $\gamma = 3$. Because the two cases agree only for small ka, which implies small $\beta_\perp/\beta_z$, only the portion of the dashed curves where β_z is nearly β is reliable. Here, $\beta = 0.943$ and if β_z is appreciably less than β, it can only be that $\beta_\perp$ has become substantial at the expense of β_z, so that ka is large and the basis for use of the unrealizable-wiggler model is not valid.

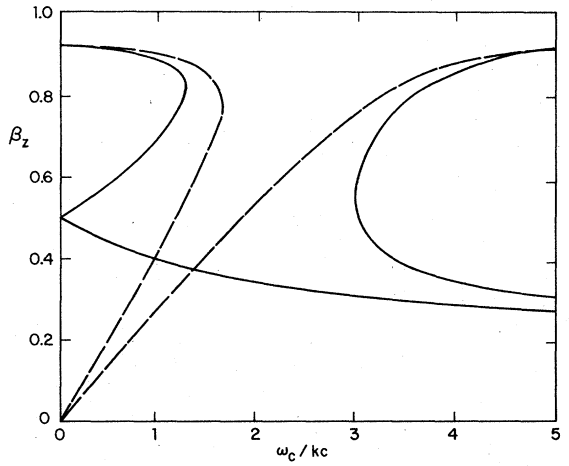

FIG. 4. Axial velocity vs guide magnetic field, for fixed energy $\gamma = 3$ and pump strength $\omega_0/kc = 0.5$, for the realizable (solid) and unrealizable (dashed) wigglers.

For practical free-electron lasers, ka will not exceed ~1 because of excessive coil current requirements[16] and reduced output frequency upshift[11] when the axial velocity becomes too low, but ka will also not be made too small because the gain of the laser increases with the quiver velocity. For highly energetic beams (large γ and g), ka will remain quite low.

IV. TRANSIENTS AND STABILITY IN WIGGLERS

A. Linearization

The helical orbits of unrealizable and realizable combinations of wiggler and uniform guide fields found above are equilibrium electron orbits. They are the trajectories of an undisturbed electron whose initial position and velocity conform exactly to the predicted helical orbit. An investigation of the response of an electron to small disturbances of these orbits can answer several important questions. Among these are the stability of the equilibria, a determination of which of the several possible equilibria for given energy and pump strength can be expected to develop, the transient development from given launch conditions different from the perfect helical ones, the natural frequencies of the system, and even the corrections to the unrealizable-wiggler orbits imposed by the axial field or transverse gradient of the realizable version or the harmonics that accompany practical source windings.

The approach taken herein is to consider realizable and practical combinations of wigglers and guide fields as the superposition of a simple unrealizable-wiggler and guide field and a small correction field. Perturbation theory is applied by linearizing the equations of motion about the unrealizable-wiggler helical orbit. The gradient of the wiggler field enters into the perturbation equations and is not negligible. The corrections to the unrealizable field, the deviations of the initial conditions from those that conform exactly to the

equilibrium orbit, and the harmonics generated by the source winding can all be treated as perturbations of the unrealizable-wiggler system under appropriate smallness conditions.

Let the unrealizable-wiggler electron orbit, given in Eq. (45), be $\vec{r}^0(\tau)$ and let it be perturbed to

$$\vec{r}(\tau)=\vec{r}^0(\tau)+\vec{s}(\tau)\,. \tag{75}$$

The accompanying perturbations in velocity and acceleration are then $d\vec{s}/d\tau$ and $d^2\vec{s}/d\tau^2$; τ is the proper time, as before. The magnetic field that affects the electron differs from the unrealizable field in Eq. (44) not only because of the correction for realizability as in Eqs. (18)–(20) and the harmonics in Eqs. (37)–(39), but also because it is to be evaluated at a perturbed location, Eq. (75). The field seen by the electron is

$$\vec{B}(\vec{r}^0+\vec{s})=\vec{B}^0(\vec{r}^0)+\vec{B}'(\tau)\,, \tag{76}$$

where

$$\vec{B}'=[\vec{B}^0(\vec{r}^0+\vec{s})-\vec{B}^0(\vec{r}^0)]+\Delta\vec{B}(\vec{r}^0+\vec{s}) \tag{77}$$

includes both the change in the unrealizable field due to the displacement of the orbital point and all the corrections to the field, fundamental and harmonics, evaluated at the displaced location. Substituting into the equation of motion, Eq. (40), and subtracting the unperturbed portions leaves the following equation for the orbital perturbation $\vec{s}(\tau)$,

$$\frac{d^2\vec{s}}{d\tau^2}=\frac{e}{m}\vec{B}^0(\vec{r}^0)\times\frac{d\vec{s}}{d\tau}+\frac{e}{m}\vec{B}'\times\frac{d\vec{r}^0}{d\tau}+\frac{e}{m}\vec{B}'\times\frac{d\vec{s}}{d\tau}\,. \tag{78}$$

This equation is exact but nonlinear, since $\vec{B}'$ depends on $\vec{s}(\tau)$.

In recognition of the smallness of $\vec{B}'$ compared to $\vec{B}^0$ if the electron is not too far from the axis, the displacement may be considered small and the equation of motion linearized about the unperturbed state. Quantities of the order of $\vec{s}$ are to be considered first-order, as are also the small correction fields $\Delta(e/m)\vec{B}=\omega_0\vec{\Omega}$ as in Eq. (32). Second-order quantities are to be neglected and, to be consistent, the last term in (78) must be considered second-order, being a product of two small quantities. By this same consistency requirement, the already small correction field $\Delta\vec{B}$ in (77) need only be evaluated along the unperturbed orbit $\vec{r}^0(\tau)$. Finally, the change in the unrealizable field that accompanies the displacement $\vec{s}$ may be replaced by the first term of the Taylor series, the one linear in $\vec{s}$:

$$\vec{B}^0(\vec{r}^0+\vec{s})-\vec{B}^0(\vec{r}^0)=\vec{s}\cdot\vec{\nabla}\vec{B}^0(\vec{r}^0)\,. \tag{79}$$

The linearized equation of motion for the displacement $\vec{s}(\tau)$ is therefore

$$\frac{d^2\vec{s}}{d\tau^2}=\frac{e}{m}\vec{B}^0(\vec{r}^0)\times\frac{d\vec{s}}{d\tau}+\vec{s}\cdot\vec{\nabla}\left(\frac{e}{m}\vec{B}^0(\vec{r}^0)\right)\times\frac{d\vec{r}^0}{d\tau}$$
$$+\omega_0\vec{\Omega}(r^0)\times\frac{d\vec{r}^0}{d\tau}\,. \tag{80}$$

The three terms on the right involve, respectively, the original unrealizable field, its gradient, and the correction fields, due to realizability and to harmonics, all evaluated along the original, unperturbed helical orbit.

B. Solution

The linearized Eq. (80) is the basic relation that yields information on transient trajectories from given initial conditions and on the stability of equilibrium orbits. Note that it is a second-order differential equation, despite the fact that the original equation of motion, Eq. (40), appears to be first order in velocity. This is due to the fact that the displacement couples to the field gradient, which can not be neglected.

To solve the vector differential equation, whose coefficients are time varying, a transformation is made to a coordinate system that conforms to the unperturbed orbit. Simultaneously, the quantities are nondimensionalized. The proper time τ is normalized to the Doppler-shifted spatial frequency, as $T=ku\tau$, and the displacement to the fundamental wiggler period, as

$$k\vec{s}=S_1\hat{w}(T)+S_2\hat{z}\times\hat{w}(T)+S_3\hat{z}\,. \tag{81}$$

Similarly, the forcing function becomes

$$\vec{\Omega}(\vec{r}^0)=\Omega_1\hat{w}(T)+\Omega_2\hat{z}\times\hat{w}(T)+\Omega_3\hat{z}\,. \tag{82}$$

The unrealizable-wiggler field is a function of z alone and its gradient is a tensor

$$\nabla[(e/m)\vec{B}^0(\vec{r})]=\omega_0 k\hat{z}[\hat{z}\times\hat{w}(T)]\,. \tag{83}$$

The normalized time derivatives in the wiggler coordinate system appear as in

$$\frac{d(k\vec{s})}{d(ku\tau)}=\left(\frac{dS_1}{dT}-S_2\right)\hat{w}+\left(\frac{dS_2}{dT}+S_1\right)\hat{z}\times\hat{w}+\frac{dS_3}{dT}\hat{z}\,, \tag{84}$$

because of the time dependence of the rotating vector $\hat{w}(T)$. The transformed equation then becomes a linear, constant-coefficient differential equation for the three-component vector S:

$$\frac{d^2S}{dT^2}+A\frac{dS}{dT}+BS=C\Omega(T)\,. \tag{85}$$

The matrices A, B, C are constants

$$A = \begin{bmatrix} 0 & (w_c - 2) & 0 \\ -(w_c - 2) & 0 & w_0 \\ 0 & -w_0 & 0 \end{bmatrix}, \tag{86}$$

$$B = \begin{bmatrix} (w_c - 1) & 0 & -w_0 \\ 0 & (w_c - 1) & 0 \\ -w_0 & 0 & -w_0 ka \end{bmatrix}, \tag{87}$$

$$C = w_0 \begin{bmatrix} 0 & 1 & 0 \\ -1 & 0 & -ka \\ 0 & ka & 0 \end{bmatrix}, \tag{88}$$

where $w_c = \omega_c/ku$ and $w_0 = \omega_0/ku$ are the normalized cyclotron frequencies of the guide and wiggler fields. The matrices A and C are antisymmetric and B is symmetric. They are known, once the equilibrium orbit has been found. For given electron energy $g = \gamma\beta kc/\omega_c$ and pump strength $p = \omega_0/\omega_c = w_0/w_c$, this entails solving Eq. (51) with Eq. (55), or

$$1 + p/ka = g(1 + k^2a^2)^{-1/2} = 1/w_c, \tag{89}$$

which then determines all the matrices.

In the standard manner, the solution to Eq. (85) entails finding the eigenvalues of the 6×6 matrix D formed from A, B and the 3×3 unit matrix I as

$$D = \begin{bmatrix} A & B \\ -I & 0 \end{bmatrix}, \tag{90}$$

in conformity with the normal, first-order form of Eq. (85),

$$\frac{dR}{dT} + DR(T) = Q\Omega(T), \tag{91}$$

where the 6-component vector R is comprised of dS/dT and S and where the 6×3 matrix Q is composed of C and the zero matrix. The solution is generated by the matrix $\exp(-DT)$, whose evaluation is straightforward, once the eigenvalues of D are known. Alternatively, Eq. (91) may be Laplace transformed to yield an algebraic solution

$$R(s) = (s + D)^{-1}[R_0 + Q\Omega(s)], \tag{92}$$

where $R(s)$ and $\Omega(s)$ are the transforms of $R(T)$ and $\Omega(T)$, and where R_0 is the initial value $(T = 0)$ of the velocity displacement vector $R(T)$. With this approach, what is needed is the matrix $(s + D)^{-1}$, which is the Laplace transform of $\exp(-DT)$.

The requirement of finding the eigenvalues of D can be simplified by resorting to the Cayley-Hamilton theorem. It is readily verified that the matrix D satisfies

$$D^2(D^2 + 1)(D^2 + \alpha^2) = 0, \tag{93}$$

where

$$\alpha^2 = (w_c/ka)^2 p(p - k^3a^3). \tag{94}$$

This reveals at once that the eigenvalues of D are 0, 0, $\pm i$, and $\pm i\alpha$, or that the natural frequencies of the system in the wiggler's rotating frame of reference are 0, 1, and α, when normalized to ku and expressed in terms of the proper time τ. The last of these, α, agrees with Friedland's[11] natural resonance frequency, μ.

Using Eq. (93), or invoking Sylvester's theorem, the required matrix inversion is easily expressed as

$$(s + D)^{-1} = E_\alpha \frac{s - D}{s^2 + \alpha^2} + E_1 \frac{s - D}{s^2 + 1} + E_0 \frac{s - D}{s^2}, \tag{95}$$

where the constant matrix coefficients are

$$E_\alpha = D^2(D^2 + 1)/[\alpha^2(\alpha^2 - 1)], \tag{96}$$

$$E_1 = D^2(D^2 + \alpha^2)/(1 - \alpha^2), \tag{97}$$

$$E_0 = (D^2 + \alpha^2)(D^2 + 1)/\alpha^2. \tag{98}$$

This effectively completes the general solution to the linearized equation because substitution of Eq. (95) into Eq. (92) yields the Laplace transform of the velocity/displacement vector $R(T)$, for any initial conditions R_0, given the correction field $\Omega(T)$ or its Laplace transform $\Omega(s)$. Before proceeding with the inverse Laplace transformations, however, much can be learned about the system's stability by examining its eigenvalues.

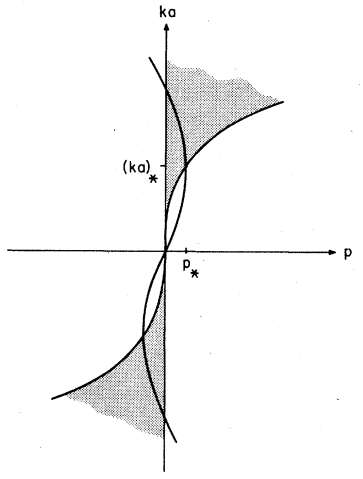

FIG. 5. Region of strong instability in the ka -p plane, shown shaded, with a typical branch of the equilibrium relation for $g > 1$. The segments $(g^{2/3} - 1)^{1/2} < |ka| < (g^2 - 1)^{1/2}$ are exponentially unstable equilibria.

C. Stability

The normalized, complex frequencies of the unforced system under small perturbations have been shown to be 0, 1, and α. The first question is then whether α is real, implying oscillation, or imaginary, corresponding to exponential growth or damping. From Eq. (94), α is imaginary if the product $p(p-k^3a^3)$ is negative. In the ka versus p plots of the characteristic Eq. (89) for the equilibrium state, this region of instability is confined to the area between the ka axis and the $p=k^3a^3$ curve, as shown shaded in Fig. 5.

The characteristic equilibrium curve does traverse the region of exponential instability if $g>1$, beyond magnetoresonance. There is then a portion of the positive helicity branch that represents unstable equilibria. It extends from the peak point at $(ka)_*=(g^{2/3}-1)^{1/2}$ as in Eqs. (58)–(59) to the intercept at $ka=(g^2-1)^{1/2}$. It should be recalled that the equilibrium is that of an unrealizable wiggler, so that ka must be kept small for the results to be reliable, although the linearized treatment does provide the first-order correction when ka becomes appreciable. This condition means that the instability region is as shown when the wiggler is operated close to, but beyond, magnetoresonance, $g \gtrsim 1$. The unstable branch was reported by Friedland,[11] without qualification regarding the size of ka.

In the region of real α, the perturbation is a sinusoidal oscillation at normalized frequency α, without damping. This natural response occurs, however, in the frame of the rotating vector $\hat{w}$, whose own frequency is unity, so that in the frame of the observer, this response will appear at normalized frequencies $\alpha \pm 1$, not at α. This is a consequence of the inherent nonlinearity of the equations of motion, which was disguised by the transformation to the rotating frame. In terms of the observer's time t, the actual natural frequencies of this oscillatory mode are $(\alpha \pm 1)ku/\gamma$. For the typical case of $g=0.928$ and $p=0.05$ discussed earlier, the values of α are 0.22 for $ka=-0.379$ and $\alpha=2.075$ for $ka=-0.0259$.

Of the other four eigenvalues, two correspond to oscillations at unit frequency, which is the same as the rotation frequency of $\hat{w}(T)$, so that this mode would combine with the rotating frame to double the frequency and also rectify it to a constant displacement. Most important, however, is the double null eigenvalue, which implies a secular growth, linear in time. This mode is weakly unstable, in the sense that it grows without bound but only linearly, not exponentially. When combined with the rotating frame, this mode appears as a growing spiral. Unless this mode is suppressed, it renders all equilibria at least weakly unstable.

D. Transient orbits

The complete solution for the perturbation of a selected equilibrium orbit is contained in the inverse Laplace transform of Eq. (92). The factor $(s+D)^{-1}$ is given as an explicit function of the Laplace transform parameter s in Eq. (95) and is simply a combination of the transforms of trigonometric functions of αT and T and of a constant and a linear ramp function; for α imaginary, the trigonometric functions become hyperbolic. The remainder of Eq. (92) involves the initial velocity deviation and displacement, in R_0, and the correction field Ω, evaluated along the unperturbed orbit and Laplace transformed.

The six-component initial-state vector R_0 is composed of $dS(0)/dT$ and $S(0)$, in the coordinate system $\hat{w}, \hat{z}\times\hat{w}, \hat{z}$ which is identical at $T=0$ to $\hat{x}, \hat{y}, \hat{z}$. Since the electron energy is fixed by γ, only its initial direction need be specified, not its speed. If the initial direction is along $\hat{v}$, so that $d\vec{r}(0)/d\tau=\gamma\beta c\hat{v}$, while the initial direction of the unperturbed orbit is, by Eq. (46),

$$\hat{n}=(\hat{z}-ka\hat{x})/(1+k^2a^2)^{1/2}, \tag{99}$$

then

$$\gamma\beta c\hat{v}=u(1+k^2a^2)^{1/2}\hat{n}+ud S(0)dT \tag{100}$$

so that the first half of the R_0 vector is given by the rectangular components of

$$\frac{dS(0)}{dT}=(1+k^2a^2)^{1/2}(\hat{v}-\hat{n}). \tag{101}$$

To specify the second half of R_0, which is $S(0)$, note from Eq. (45) that the initial position of the unperturbed orbit is $\vec{r}^{\,o}(0)=\vec{r}_0+a\hat{y}$, where $\vec{r}_0$ locates the guiding center. The latter is arbitrary for the unrealizable wiggler and could be selected to keep the magnitude of the perturbation as small as possible, so as to validate the linearized analysis over a wider range. It is advantageous, however, to specify the arbitrary location of the guiding center of the unperturbed orbit as the coordinate origin. This ascribes any deviation from an axicentered helix to the perturbation but also makes both r and ϕ-kz constants of the motion along the equilibrium orbit. This achieves an enormous simplification of the forcing function, as will be seen. With this choice, the rest of the R_0 vector is given by

$$S(0)=k\vec{r}(0)-ka\hat{y}, \tag{102}$$

in rectangular coordinates.

The last term in Eq. (92) involves the Laplace transform of the correction field $\vec{\Omega}(T)$, due to realizability and harmonics of the source winding, expressed in the $\hat{w}, \hat{z}\times\hat{w}, \hat{z}$ coordinate system as in Eq. (82). The great advantage of axicentered un-

perturbed orbits is that $\vec{\Omega}(T)$ becomes merely a constant vector $\vec{\Omega}_0$, as is clear from Eq. (32), where kr is fixed at ka and $\phi - kz$ is fixed at $\pi/2$. The Laplace transform in Eq. (92) is then $\Omega(s) = \Omega_0/s$ and the three components of Ω_0 are $-\Omega_\phi(ka,\pi/2)$, $\Omega_r(ka,\pi/2)$ and $\Omega_z(ka,\pi/2)$. More explicitly, as in Eqs. (33)–(39), the vector is

$$\Omega_0 = \Omega_0^1 + \sum_{n>1} \Omega_0^n , \tag{103}$$

with

$$\Omega_0^1 = \begin{bmatrix} I_0(ka) - 1 - I_2(ka) \\ 0 \\ 2I_1(ka) \end{bmatrix} , \tag{104}$$

for the ideal realizable wiggler or the fundamental component for any winding, and

$$\Omega_0^n = \xi_n Q_n \begin{bmatrix} [I_{n-1}(nka) - I_{n+1}(nka)]\sin n\pi/2 \\ [I_{n-1}(nka) + I_{n+1}(nka)]\cos n\pi/2 \\ 2I_n(nka)\sin n\pi/2 \end{bmatrix} , \tag{105}$$

for its harmonics.

The only remaining task is to invert the elementary Laplace transforms in Eq. (92), using Eq. (95), or simply

$$R(s) = \sum_\lambda \left(\frac{s-D}{s^2+\lambda^2} E_\lambda R_0 + \frac{s-D}{s(s^2+\lambda^2)} E_\lambda Q \Omega_0 \right), \tag{106}$$

to obtain $R(T)$, which includes both the dS/dT and $S(T)$ perturbations, as explicit functions of time. In Eq. (106), $\lambda = \alpha$, 1, and 0 and the fact that the E_λ and D matrices commute has been used. For the real and nonzero values of λ, the inverse transforms are $\cos\lambda T$, $\sin\lambda T/\lambda$, and $(1-\cos\lambda T)/\lambda^2$; for the case of imaginary α, the functions become hyperbolic; for $\lambda = 0$, the time functions are the polynomial forms $1, T, T^2/2$.

Exclusive of the branch of the characteristic equation corresponding to imaginary α and hence exponentially unstable equilibria, the response to small disturbances is seen to involve oscillatory, undamped motion, except for the terms involving $\lambda = 0$ in Eq. (106). The latter include functions growing in time as T and T^2 in the rotating coordinate system, which appear as spirals of increasingly large radius in the stationary frame. They represent a weak, nonexponential instability or secular growth of the orbits. Upon closer examination, however, it is found that the quadratic time factor $T^2/2$ is actually innocuous. This is because its coefficient $DE_0Q\Omega_0$ in Eq. (106) vanishes identically. The matrix DE_0Q is zero, a consequence ultimately of the fact that the two submatrices B,C in Eqs. (87)–(88) both annihilate the same eigenvector. Consequently, the secular behavior never includes a disturbance that grows quadratically in time. However, the linear growth factor is active, both in response to the initial conditions R_0 and to the field corrections Ω_0, and renders the equilibria weakly unstable even when α is real.

For given electron energy and pump strength parameters g,p it is a simple matter to find the equilibrium values of ka and w_c from Eq. (89) and evaluate the matrices A,B,C in Eqs. (86)–(88), then D and, with the natural frequency α obtained from Eq. (94), to compute the three matrices E_λ in Eqs. (96)–(98), as well as DE_λ, $E_\lambda Q$, and $DE_\lambda Q$. The minimal corrections to the unrealizable wiggler are contained in Ω_0^1 of Eq. (104) for an ideal wiggler free of harmonics, whereupon the vectors $E_\lambda Q\Omega_0^1$ and $DE_\lambda Q\Omega_0^1$ can be evaluated. For a practical wiggler with arbitrary source winding specified by the Fourier series coefficients Q_n in Eq. (28), the harmonics in Eq. (105) may be added to Ω_0^1 to arrive at the Ω_0 vector for any wiggler. Also, from the initial location $\vec{r}(0)$ and direction of motion $\hat{v}$ of the electron, the vector R_0 can be formed by Eqs. (101)–(102) and $E_\lambda R_0$ and $DE_\lambda R_0$ evaluated. All these constant coefficient vectors are combined with the oscillatory (or hyperbolic) and secular time functions given above to arrive at the perturbation vector $R(T)$, which gives both the orbital velocity and trajectory deviations from the selected equilibrium orbit. The last step in tracing the disturbed orbit is to restore both the equilibrium helix and the rotating coordinates to arrive at the electron trajectory from given launch conditions in a specified wiggler system, in the form

$$kx(T) = -ka\sin T + R_4(T)\cos T - R_5(T)\sin T , \tag{107}$$

$$ky(T) = ka\cos T + R_4(T)\sin T + R_5(T)\cos T , \tag{108}$$

$$kz(T) = T + R_6(T) , \tag{109}$$

with $T = ku\tau = kut/\gamma = (1+p/ka)\omega_c t/\gamma$. The products of trigonometric functions in Eqs. (107)–(108) generate combination frequencies $\alpha \pm 1$, frequency doubling to 2, and rectification to a constant displacement, besides the growing oscillations of the form $T\cos T$ and $T\sin T$.

Figure 6 shows the projection onto a transverse plane of the orbit of an electron in an ideal wiggler with the typical parameters previously cited $g = 0.928$, $p = 0.05$, and $ka = -0.379$. Its initial position was chosen as $k\vec{r}(0) = -0.3\hat{y}$ and its initial direction was $\hat{v} = \hat{z}$, exactly parallel to the axis. In the absence of the wiggler, the electron would simply continue uniformly, parallel to the axis at its initial radial displacement. Thus, the wiggler does serve to impart a transverse undulation to the electron. The radial oscillations are evident

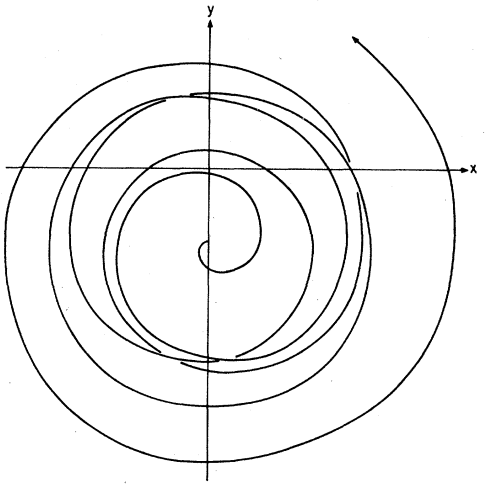

FIG. 6. Transverse projection of electron trajectory, from initial position $ky = -0.3$ with initial velocity along the axis, for guide and wiggler parameters $g = 0.928$ and $p = 0.05$, based on the equilibrium quiver parameter $ka = -0.379$. The weak instability becomes evident after about five axial periods of the wiggler.

in the figure. The time-averaged transverse position, or guiding center, is found at $-0.31\hat{y}$ but it is also clear that the electron spirals outward, as predicted. After four or five periods of the wiggler, the electron has reached points far enough from the equilibrium radius $|ka| = 0.379$ to make the linearized analysis doubtful.

The features illustrated in this figure, of oscillations superimposed on a gyration with the eventual dominance of the unbounded outward spiraling, are typical of the results for general initial conditions, although the oscillation frequencies and the rate of growth of the spiral may vary over wide limits.

E. Bounded orbits

The tendency of an electron to spiral outward in a wiggler is a consequence of the participation of the null eigenvalue of D in the solution, Eq. (106), for the perturbed orbit, leading to disturbances growing as T. If the coefficient of that linearly growing perturbation mode could be made to vanish, the remaining disturbance would be merely oscillatory (assuming real α) and the orbit would remain bounded. Examination of Eq. (106) shows that for the secular behavior to be eliminated the vectors DE_0R_0 and $E_0Q\Omega_0$ must be made equal. In fact, these two six-component vectors are always proportional to a single eigenvector, which depends only on ka, so that just one condition on a combination of initial positions and velocities need be satisfied to suppress the linearly growing mode.

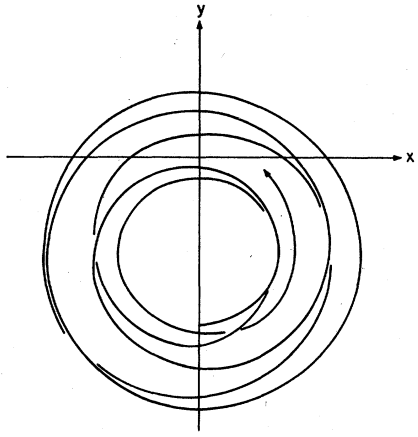

FIG. 7. Transverse projection of a bounded-electron trajectory, from initial position $ky = -0.636$ and axial initial velocity, for the same equilibrium helix as in Fig. 6. The weak instability is suppressed. The realizable-wiggler corrections are for an ideal one, without harmonics.

The ratio, h, of a nonzero component of $E_0Q\Omega_0$ to the corresponding component of the eigenvector of DE_0 is predetermined by the equilibrium orbit parameters and the combination of initial conditions in DE_0R_0 involves only $ky(0)$ and $\hat{v}\cdot\hat{n}$. There is therefore a class of bounded orbits, conforming to the condition

$$ky(0) = h + ka + (ka + 1/ka)(1 - \hat{v}\cdot\hat{n}), \tag{110}$$

which suffices to suppress the secular behavior.

Figure 7 shows the orbit of an electron launched in the axial direction for the same parameters as for Fig. 6, except that the initial location is at $k\vec{r}(0) = -0.636\hat{y}$ instead of $-0.3\hat{y}$, in accordance with the bounded orbit condition, Eq. (110). It is clear that the secular behavior has been suppressed, leaving only the oscillations.

If, in addition to satisfying the bounded orbit condition Eq. (110), the initial direction is chosen to be $\hat{n}$, then the oscillations are also suppressed and what remains is a perfect helix, with a fixed radius

$$(ka)' = ka + h, \tag{111}$$

representing a correction to the radius predicted for an unrealizable wiggler. The ratio h of vector $E_0Q\Omega_0$ to the eigenvector of DE_0 is a function of g,p.

To illustrate the influence of harmonics generated by a practical winding of a realizable wiggler, Fig. 8 presents the bounded orbit for axial initial velocity for the same equilibrium as in Fig. 7 but with the initial position now required to be at $k\vec{r}(0) = -0.648\hat{y}$ instead of -0.636 in order to suppress the unbounded motion, when the harmonics of a

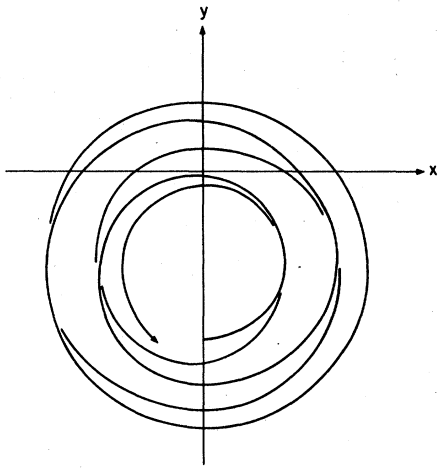

FIG. 8. Bounded-electron trajectory in the field of a bifilar helix at $kb = 1.5$, for the same parameters as in Fig. 7, but now with initial position $ky = -0.648$ to suppress the linear growth. Harmonics 3 to 11 are included.

bifilar wiggler winding are taken into account. The winding was taken to be at $kb = 1.5$ and harmonics 3, 5, 7, 9, and 11 were included, besides the fundamental; higher harmonic contributions are negligible in this case. It appears that the effects of harmonics introduced by practical versions of the wiggler are noticeable but not major.

V. CONCLUSIONS

The fact that the unrealizable-wiggler field violates Maxwell's equations can not be dismissed as an insignificant flaw of the theories of the free-electron laser for which this field has become the canonical model. It lacks both the periodic axial field component and the radial variation of the entire field that are inescapable features of realizable versions of the undulator. These affect the motion of electrons in the wiggler and, in most practical cases, result in appreciably different transverse velocities and sizes of the equilibrium helical orbits.

The gain of the free-electron laser depends on the quiver motion imparted to the electrons by the wiggler. One measure of that undulation, the ratio of transverse to axial velocities, has been shown to be the same parameter, ka, that measures the size of the helical orbit and how far from the axis the electron travels. Calculations based on the unrealizable wiggler are reliable only if the normalized radial excursion kr is small but the wiggler serves its purpose of imparting a substantial quiver to the electrons when ka is not small. This contradiction in the requirements on the quiver parameter is central to the question of whether the unrealizable wiggler can be a reliable basis for analyzing the free-electron laser.

A helical orbit is found to be a steady-state trajectory for an electron even in a realizable wiggler, by following the locus of vanishing radial field. There are, however, two important differences from the case of the unrealizable wiggler. The first is that the size of the helix and the quiver velocity are different from the ones expected for the corresponding unrealizable version, as soon as ka becomes appreciable. As ka increases, both the axial field and the radial gradient tend to enhance the contribution of the pump field to the axial motion, in relation to that of the uniform guide field, instead of letting it diminish, as for the unrealizable wiggler. The second major difference is that a helical equilibrium orbit can exist only for sufficiently low pump strengths. For stronger wigglers, the electron's energy becomes insufficient to support a helical trajectory. This is a consequence of the radial variation of the field; the unrealizable wiggler allows a helical orbit for any pump strength.

The perturbation analysis of the helical equilibria of the unrealizable wiggler reveals information about the response of the system to small disturbances, about its stability, about the effects of harmonics of practical wiggler windings, and about the transient development of an electron trajectory from given initial conditions. In the coordinate system that rotates with the wiggler field, two natural frequencies of oscillation are found. One is just the rate at which the period of the wiggler is traversed by the axial motion of the electron. The other depends in a more elaborate way on the wiggler parameters and can even turn into an exponential instability instead of an oscillatory response. In the laboratory frame, combination frequencies are observed, in addition to these natural ones.

The linearized analysis also reveals a secular behavior of the disturbances that are not exponentially unstable. This arises from a double null eigenvalue of the system, implying that the perturbations tend to grow linearly in time. Thus, the wiggler induces outwardly spiraling motion in general. The equilibrium orbits are hence either strongly or weakly unstable. In the latter case, the secular growth can be shown[17] to reduce to a large but bounded deviation on a long time scale but, in practical cases, the electron would strike the wall of the drift tube before turning around.

With arbitrary launch conditions treated as small deviations from the initial conditions that would keep the electron on the nearest steady-state helix, the perturbation analysis yields the motion of an electron that starts at a given location with

a given initial direction. In particular, an initial velocity parallel to the uniform guide field is seen to become converted into a mixture of transverse and axial oscillations at the expense of the axial drift, as the wiggler imparts a quiver motion to the electron. The weak instability, however, soon imposes an outwardly spiraling, growing gyration that eventually dominates the bounded oscillation.

The analytic solution also reveals a condition on the initial position and direction that can suppress the secular behavior. There is then a class of bounded nonhelical orbits, with oscillatory but nonsecular response. This suggests attempting to shape the cathode to favor that class of electron trajectories and keep the electrons from spiraling away too soon. The results are clearly relevant to beam spreading and beam quality in free-electron lasers.

ACKNOWLEDGMENT

This work was supported by AFOSR under Contract No. 80-0118.

[1]P. Sprangle, R. A. Smith, and V. L. Granatstein, in *Infrared and Millimeter Waves*, edited by K. Button (Academic, New York, 1979), p. 279.
[2]J. P. Blewett and R. Chasman, J. Appl. Phys. 48, 2692 (1977).
[3]T. Kwan, J. M. Dawson, and A. T. Lin., Phys. Fluids 20, 581 (1977).
[4]N. M. Kroll and W. A. McMullin, Phys. Rev. A 17, 300 (1978).
[5]A. Hasegawa, Bell Syst. Tech. J. 57, 3069 (1978).
[6]I. B. Bernstein and J. L. Hirshfield, Phys. Rev. Lett. 40, 761 (1978).
[7]I. B. Bernstein and J. L. Hirshfield, Phys. Rev. A 20, 1661 (1979).
[8]T. Kwan and J. M. Dawson, Phys. Fluids 22, 1089 (1979).
[9]P. Sprangle and R. A. Smith, Phys. Rev. A 21, 293 (1980).
[10]P. Sprangle, C.-M. Tang, and W. Manheimer, Phys. Rev. A 21, 302 (1980).
[11]L. Friedland and J. L. Hirshfield, Phys. Rev. Lett. 44, 1456 (1980).
[12]R. C. Davidson and H. S. Uhm, Proceedings of the Sherwood Meeting, Tucson, Arizona, 1980, Paper No. 2C28 (unpublished).
[13]L. Friedland and J. L. Hirshfield (unpublished).
[14]L. Friedland, Phys. Fluids 23, 2376 (1980).
[15]I. B. Bernstein and L. Friedland (unpublished).
[16]B. M. Kincaid, J. Appl. Phys. 48, 2684 (1977).
[17]S. Johnston (private communication).